J. Exp. Biol. (1967), 46, 63–84
With 12 text-figures
Printed in Great Britain

CONDUCTION VELOCITIES AND THEIR TEMPERATURE COEFFICIENTS IN SENSORY NERVE FIBRES OF COCKROACH LEGS*

BY K. M. CHAPMAN† AND J. H. PANKHURST
Department of Physiology, University of Alberta, Edmonton, Alberta, Canada

(*Received* 6 *August* 1966)

The cockroach-leg preparation of Pumphrey (1936) and Pringle & Wilson (1952) lends itself easily to measurements of conduction velocity in afferent nerve fibres from many of the larger mechanoreceptive sensilla of the leg. Conduction velocity is a quantity that can be measured quite precisely, and it has an important bearing on several open problems involving sensory mechanisms in insects, as well as in cellular neurophysiology more generally. One group of problems relates to the sensory transfer functions for tactile spine mechanoreceptors of *Periplaneta*, determined by Pringle & Wilson (1952) and Chapman & Smith (1963). Sensory transfer functions are quantitative expressions of the stimulus–response relationship, which describe some aspects of the temporal sensory code used in information transmission, and which provide useful insight in identifying component transducer mechanisms in the sensory ending. Conduction velocity is important in this context because it contributes quantitatively to the sensory code, and because it generates a quantifiable experimental artifact in the analysis of transducer mechanisms. In the present work these effects are evaluated and are shown to be small but not negligible.

Secondly, conduction velocity provides a physiological estimate of nerve fibre diameter. Knowledge of the diameters of fibres innervating the mechanoreceptors of cockroach legs should be an important guide to future microelectrode work, and is essential in estimating current densities and related electrical properties of the sensory cell membranes. The morphological literature is somewhat confusing regarding fibre diameters. Pringle (1938) found fibres of the order of 6–15 μ arising from the campaniform sensilla of the trochanter of *Periplaneta*. On the other hand Guthrie (1962), tracing fibres in serial sections of regenerating fifth podial nerve in *Periplaneta*, found that virtually all fibres in the 5–20 μ range innervated muscle fibres, and that the remaining small nerve fibres, ranging to less that 1 μ, accounted for nearly all the sensory innervation of the leg. From this he concluded that no sensory fibre diameters exceed about 5 μ. The detailed work of Dresden & Nijenhuis (1958) on the sensory innervation of the legs of *Periplaneta* did not give fibre diameter measurements, although Nijenhuis & Dresden (1952) had described the innervation of structures later shown to be campaniform sensilla in the bases of the tactile spines (Chapman, 1965). In the

* Supported by grant MA 760 of the Medical Research Council of Canada.
† Present address: Division of Biological and Medical Sciences, Brown University, Providence, R.I., U.S.A.

latter report, the afferent nerve fibres were not visible in our histological preparations of these sensilla.

Moreover, the literature on conduction velocities of insect nerve is notably sparse (cf. reviews of Rockstein, 1965; Bullock & Horridge, 1965; Treherne & Beament, 1965). In much of the work on this subject estimation of conduction velocity has been of secondary interest, and many of the estimates include latencies other than conduction time. Further, in many studies temperature has not been specified, so that it is difficult to make meaningful comparisons between one published report and another. A number of relevant reports have been collated here relating fibre diameter and conduction velocity in a number of species (Fig. 11), to form a basis for an estimate of diameter for *Periplaneta*. Our average conduction velocity, 3·3 m./sec. at 20° C., indicates diameters of about 10 μ.

MATERIALS AND METHODS

Preparation. All work was done with adult *Periplaneta americana* of various ages, fed on rabbit chow and water, reared at 25–30° C., and transferred to room temperature (18–25° C.) a few weeks before the experiments. The essential technical details are as described previously (Chapman, 1965). Amputated mesothoracic and metathoracic legs were used throughout. These were taken high in the coxa, with carbon dioxide anaesthesia, and mounted on stainless-steel pin electrodes (Fig. 1). Most were studied in moist air, with petroleum jelly on the cut end to retard drying, but a few were immersed in paraffin oil. Nearly all the work was done with tibial tactile spines, but dorsal femoral spines were studied in a few cases, and several proprioceptive campaniform sensilla of tibial group 6 (Pringle, 1938) were used in one case. In our nomenclature, tibial spines are designated anatomically by rows (Fig. 2), and numbered from the proximal end of each row.

Stimulation recording. Mechanical stimulation was used throughout, to produce trains of impulses from individual sensilla. The precise nature of the stimulus was not critical, since the conduction velocity determination used was independent of the stimulus. Tactile spines were stimulated by small displacements with a tungsten needle or a steel insect pin held in a micromanipulator, usually with manual control, while proprioceptive campaniform sensilla were excited by contact with the tip of a fine probe. In some cases the stimulating probe was attached to a ceramic bender (Clevite PZT) driven by a low-frequency waveform generator (Hewlett-Packard 202A).

Each of two pairs of recording electrodes was connected to a differential a.c. preamplifier (Grass P-9) with 2 MΩ input impedance between electrode pairs, and nominal bandpass of 10 c./s. to 50 kc./s. in all cases. The preparation was partially shielded, and grounded only through the parallel impedance to ground of the four input terminals, effectively about 0·7 MΩ. The longitudinal resistance of three preparations, measured between the femoral recording electrodes using both bridge and shunt methods, was about 20 kΩ, so that the input impedance of the amplifiers was adequately high.

Diphasic action potentials from each pair of recording electrodes were displayed on separate traces of an oscilloscope, usually a single beam instrument with a beam splitter (Tektronix 536 and CA, respectively), or a dual beam oscilloscope (Tektronix

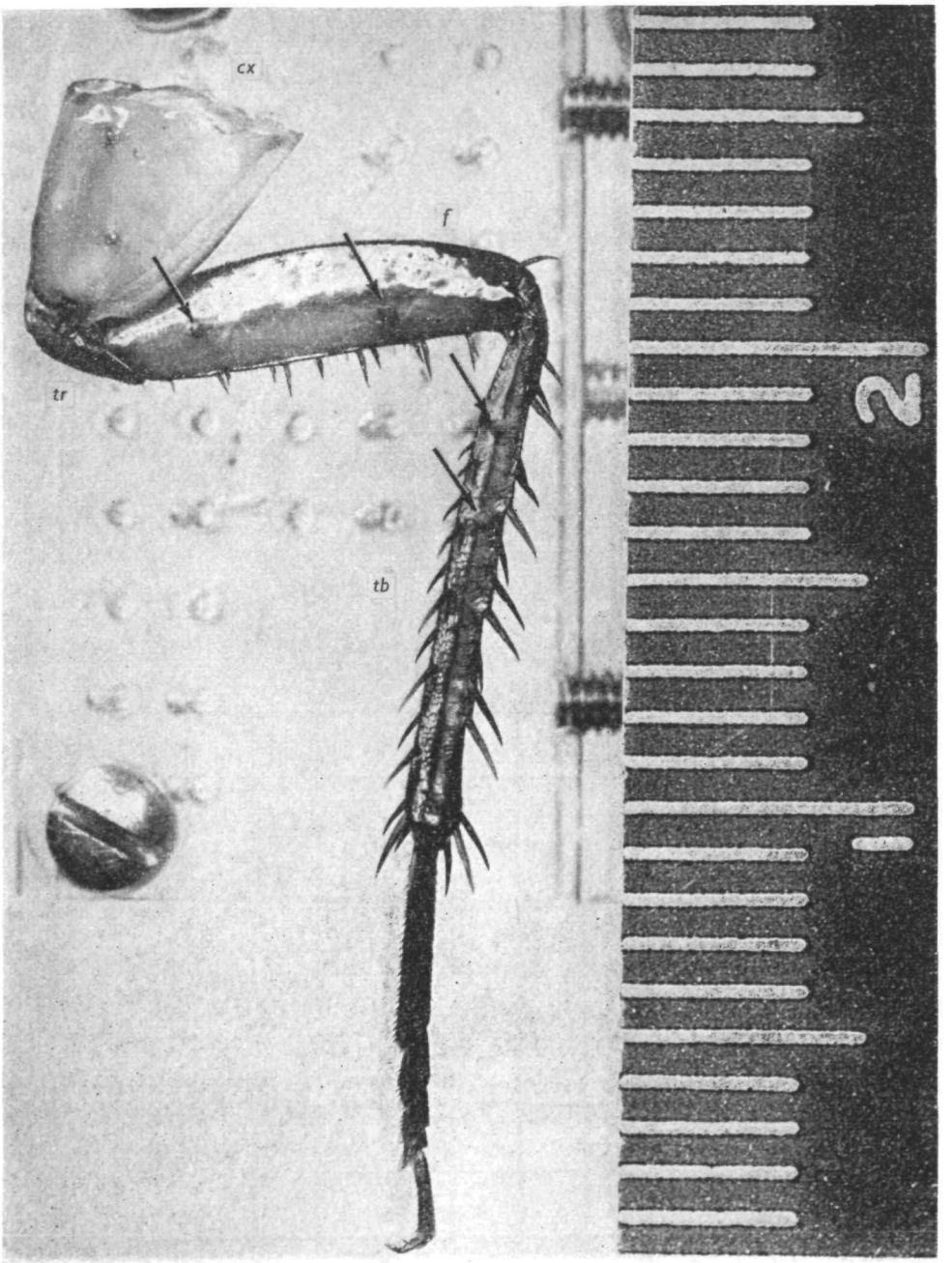

Fig. 1. Right mesothoracic leg mounted on three pairs of electrodes, posterior view. *cx*, coxa; *tr*, trochanter; *f*, femur; *tb*, tibia. Scale, cm and mm. Tibial-to-femoral conduction distance was taken as 8·75 mm. (Expt. 15).

502). In both cases the sweep speeds were calibrated with a Tektronix 181 time-mark generator, the frequency dividers of which were verified for accuracy before and during the series of experiments. In addition, the alignment of both sweeps relative to the cathode-ray tube reticle was verified from time to time.

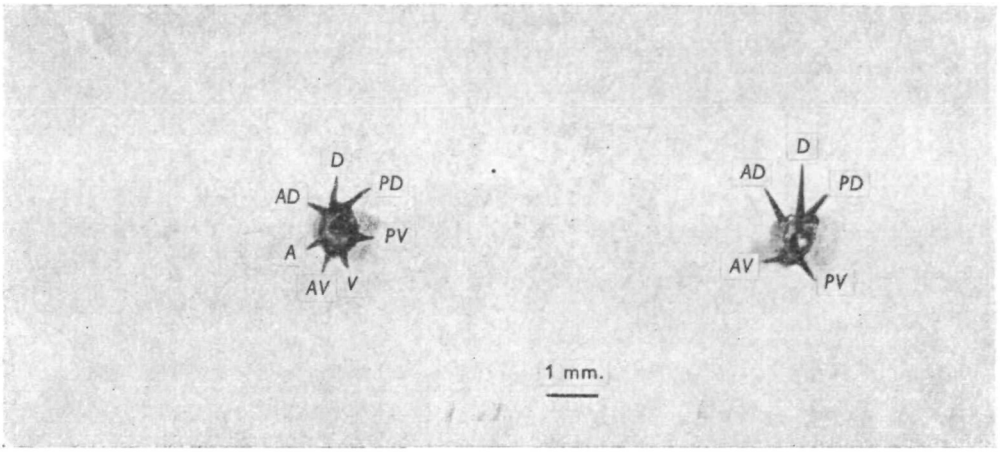

Fig. 2. Nomenclature used in designating spine rows; sections of left metathoracic tibia, pinned on to wax, viewed from distal end. Right, five rows of non-terminal spines; left, seven terminal spines. *AD*, Anterodorsal; *D*, dorsal; *PD*, posterodorsal; *PV*, posteroventral; *V*, ventral; *AV*, anteroventral; *A*, anterior. *A* and *V* occur in terminal group only.

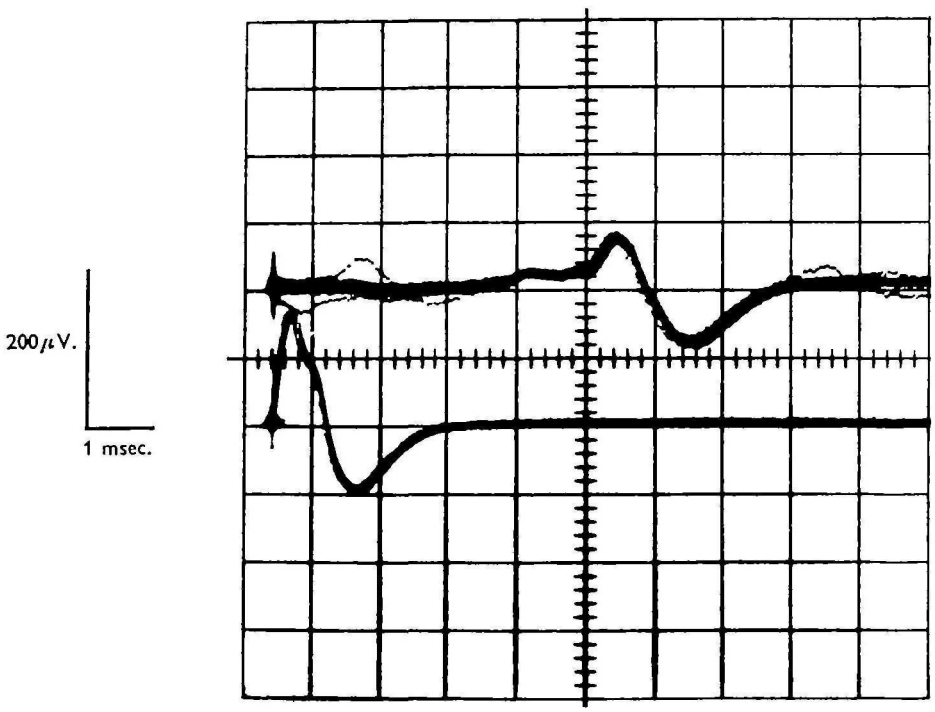

Fig. 3. Oscilloscope record indicating conduction time from distal electrodes (lower trace) to proximal electrodes (upper trace). Calibration at left; conduction distance, 15·3 mm.; velocity, 3·28 m./sec.; 13·3° C. (Expt. 5).

The two oscilloscope sweeps were triggered simultaneously as each afferent impulse approached the distal pair of recording electrodes, the initial deflexion of its diphasic action potential providing the triggering signal (Fig. 3). Thus the action potential from the distal recording site appears at the extreme left of one of the two traces, usually the lower. When the same impulse reached the proximal recording site, a second action potential was produced on the other trace, later than the first by the conduction time between the two sites. Conduction time was taken as the time-interval between the base-line crossover point of the distal diphasic action potential and that of the proximal. Usually a dozen or more impulses from one or more evoked trains were superimposed in each oscilloscope record, and several such records were averaged for each determination of conduction velocity. The method used to determine conduction velocity from the oscilloscope records is illustrated in Fig. 4, and described in detail in a later section.

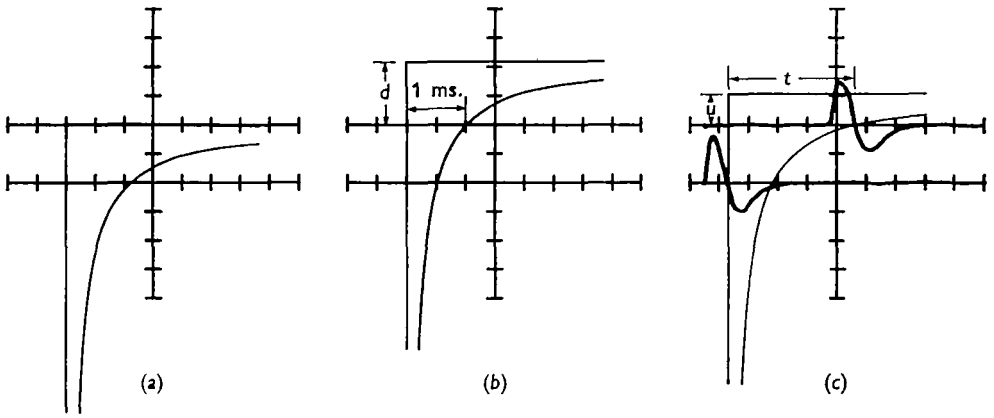

Fig. 4. Procedure for reading conduction velocity from film records with a calibrated 10-turn potentiometer, using a hyperbolic cursor carried by the movement of an $X-Y$ recorder. Each diagram shows the transparent cursor overlying an oscilloscope record, drawn schematically here for simplicity; in *a* and *b* the impulse traces have been omitted (cf. Fig. 3). (*a*) Zero setting: with the reading potentiometer set at zero, the abscissa (time axis) of the cursor is placed over the base-line of the proximal (upper) impulse trace. (*b*) Calibration: the potentiometer dial is set to the numerical value of conduction distance, *d*, in mm. and the Y-axis sensitivity of the recorder adjusted such that the cursor then delimits a 1·0 ms. interval on the proximal baseline. (*c*) Reading: with the cursor ordinate (velocity axis) intersecting the base-line crossing of the distal impulse trace, the reading potentiometer is used to translate the cursor vertically so that the hyperbola intersects the baseline crossing of the proximal trace; the potentiometer then indicates conduction velocity u in m./sec.

Electrode spacing and conduction distance. Pairs of stainless-steel insect pins serving as recording electrodes were arranged in a square array with 2 mm. spacing in a flat Perspex clamp, and the leg was mounted on them. Usually three pairs were employed, the most distal pair penetrating the upper part of the tibia, the next pair going through the femur, and the third through the coxa (Fig. 1). Most commonly the tibial and femoral pairs were chosen for recording, but occasionally the pair immediately across the femoro-tibial joint and that across the trochanter were used instead. When tibial and femoral pairs were used, the femoral pair was spaced about twice as far apart as the tibial, about 4 mm. and 2 mm. respectively, producing nearly equal action potential amplitudes from the two sites.

Conduction distance between the two recording sites was estimated as the distance from the midpoint of the distal electrode pair to that of the proximal pair. Electrode positions were measured *in situ* at the end of each experiment, with an ocular micrometer at first, but in all of the later experiments from a calibrated photograph of the preparation as in Fig. 1. No attempt was made to determine the precise course of the afferent nerve in the leg, and conduction distance has been taken arbitrarily as an average of plausible path lengths within the confines of the cuticle.

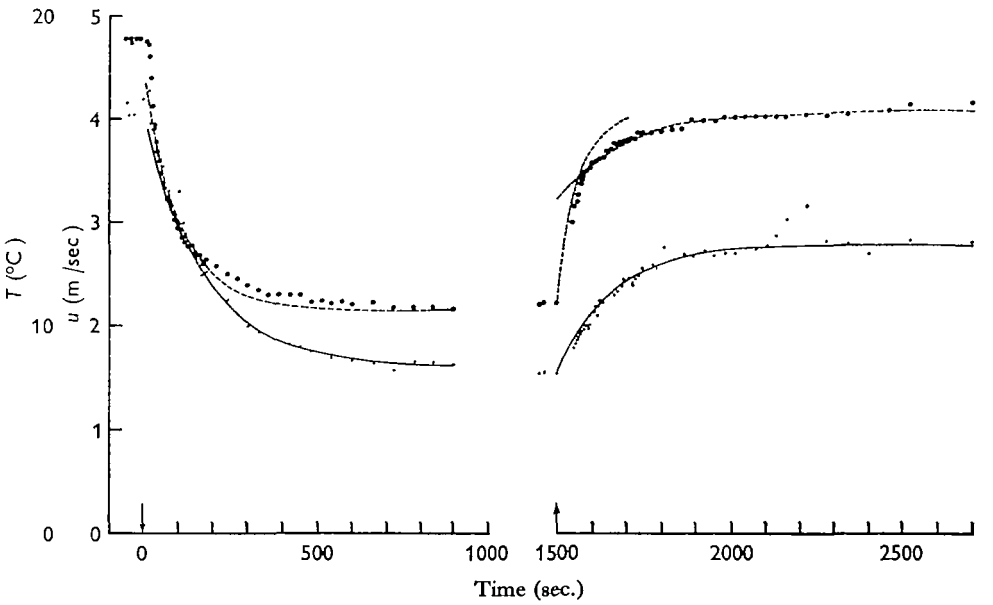

Fig. 5. Thermal equilibration curves for indicated chamber temperature T (○) and for conduction velocity u (●); curves are calculated exponential regression lines. Arrows indicate times at which the temperature of the circulating water was changed. The indicated temperature during warming was obviously not a simple exponential process and has been arbitrarily fitted piecewise with two exponentials (Expt. 16).

Temperature variation. When temperature coefficients were to be determined, preparations were enclosed within an air-filled metal chamber with hollow walls and bottom, around which water at various temperatures could be circulated. A plastic lid with holes to accommodate the necessary apparatus partially covered the top, to reduce air exchange with the surroundings.

Air temperature in the chamber was measured with a small thermistor bead placed close to the leg, operated in a bridge circuit and calibrated to within 0·1° C. with a mercury thermometer. Chamber temperature was not regulated, but was varied at convenient rates by altering the temperature and flow rate of the circulating water. Using ice water and warm tap-water, temperatures from 5 to 42° C. were attained.

Working in air was convenient for electrical insulation and for ventilating the tissue, but tended to retard thermal equilibration. To assess the latter effect, thermal transient responses of the chamber and of the preparation were studied in detail in one experiment (Figs. 5, 6). Following a sudden, substantial change in temperature of the

circulating water, it took several minutes for conduction velocity to stabilize. As one would expect, the thermistor bead equilibrated more quickly than the considerably larger leg. The time-courses of the thermal responses are shown in Fig. 5. For convenience these may be approximated as simple exponential functions of time, and in these terms the time-constant for equilibration of conduction velocity was roughly twice that for the temperature probe. (A single exponential is clearly not adequate to approximate the warming phase in Fig. 5, and separate exponentials have been fitted

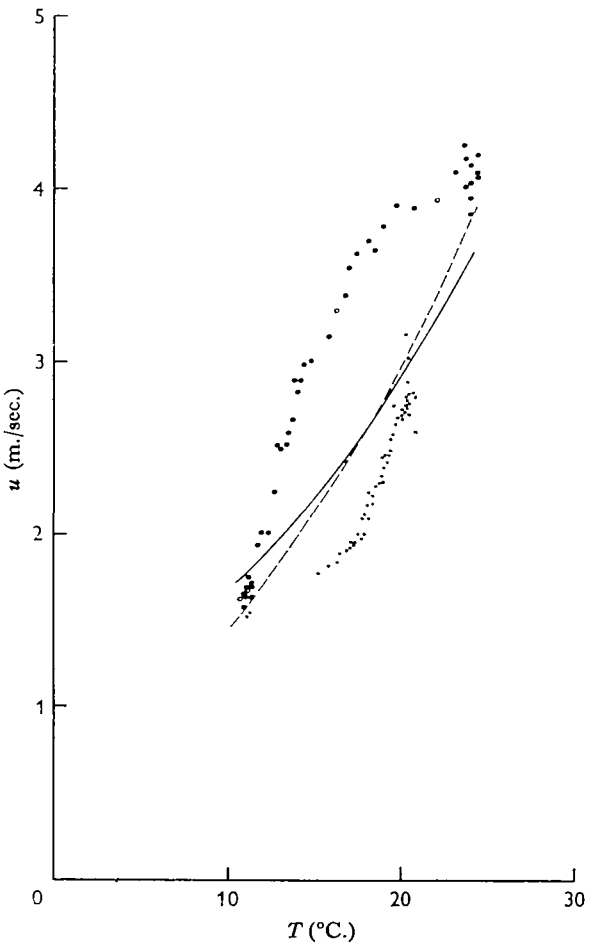

Fig. 6. Conduction velocity u as a function of indicated chamber temperature, T, data of Fig. 5, demonstrating hysteresis due to thermal lag. O, Decreasing temperature; ●, increasing temperature; —, Arrhenius equation calculated using all points; – – –, calculated using points at thermal equilibrium only.

arbitrarily to the early and late phases of equilibration.) In this situation the relationship between conduction velocity and chamber temperature contains appreciable hysteresis, reflecting the thermal lag between the preparation and the surrounding air (Fig. 6). This is a potential source of error in estimating temperature coefficients of conduction velocity, and to reduce this effect when actually determining tempera-

ture coefficients, chamber temperature changes were executed slowly, usually in complete cycles (Fig. 7). Calculation of temperature coefficients is discussed in detail below.

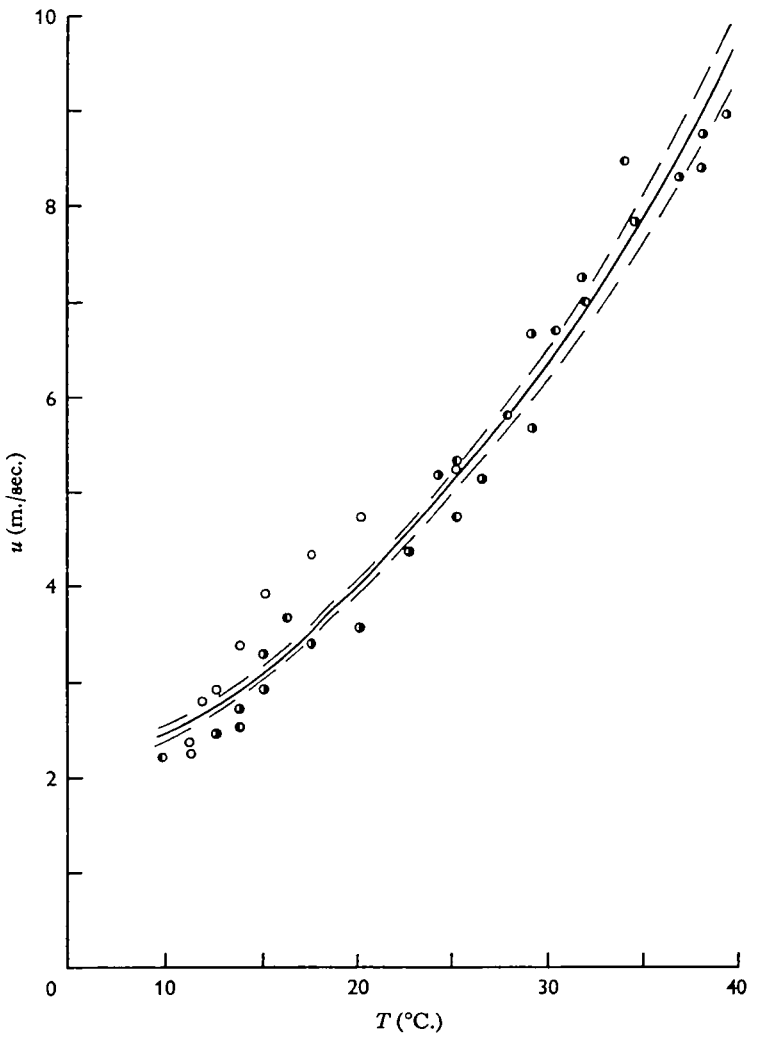

Fig. 7. As Fig. 6, but for a case in which temperature changes were executed slowly to minimize thermal hysteresis (Expt. 13). O, Initial temperature descent; ◑, rising temperature; ◐, final descent; —, Arrhenius equation calculated using all points; – – –, one standard deviation from the calculated curve.

PRINCIPLES AND COMPUTATION

Symbols. The following list defines most of the quantitative symbols used throughout the text (anatomical symbols are explained in Table 1 and Fig. 2):

B Arrhenius temperature coefficient
D Fibre diameter
d Conduction distance
L Total wavelength of action potential

L_a Wavelength of inward radial action current
Q_{10} Relative increase in conduction velocity per 10° C.
s Spacing between two electrodes of a pair; complex frequency
T Temperature (absolute unless otherwise specified)
t Conduction time
u Conduction velocity
u_{20} Conduction velocity at 20° C.
u_∞ Limiting conduction velocity in Arrhenius equation
τ Total duration of action potential
τ_a Duration of inward radial action current
ϕ Phase shift by which response leads stimulus

Conduction velocity. In principle, conduction velocity u was determined from measured conduction distance d, conduction time t and the defining equation:

$$u = d/t. \tag{1}$$

To facilitate data analysis, however, a graphical analogue technique was used to read conduction velocity directly from the oscilloscope records (Fig. 4).

The essential device for the method was a miniature nomogram of equation (1), consisting of a rectangular hyperbola and its co-ordinate axes, reduced onto transparent photographic film from a large, accurate ink drawing (Chapman, 1957). The nomogram was mounted on the pen arm of an X–Y recorder, where it served as a reading cursor which could be conveniently positioned over a strip of oscilloscope records, using the positioning controls of the X–Y recorder. The conduction-velocity scale, along the ordinate axis of the nomogram, was given by the dial of a 10-turn potentiometer. The latter was operated as a voltage divider from either a battery or a variable-voltage power supply, and fed into the Y-axis of the recorder, to provide measured vertical movement of the nomogram. The ordinate scale could thus be varied for calibration by varying either the Y-axis sensitivity of the recorder or the power supply voltage. The abscissal (time) scale was taken directly from that of the oscilloscope records, so that after calibration, when a conduction time was laid off on the abscissa, the corresponding ordinate reading gave the conduction velocity. For each leg preparation, the ordinate was calibrated using the measured conduction distance d, a convenient value of t and equation (1). Thus the ordinate reading for $t = 1{\cdot}0$ msec. was set at $u = d$/msec. (Fig. 4*b*). The procedures for calibration and for reading velocity are illustrated in detail in Fig. 4.

The precision of the method, estimated from the standard deviations of replicate velocity readings (Table 1), was about 3–4 %. Individual potentiometer readings could be made to three decimal digits, and therefore did not limit the precision. Individual variability between fibres and variations due to temperature were considerably greater than the limits of reading precision, so that the technique was adequate to study these grosser effects.

Temperature coefficients. The temperature dependence of conduction velocity in these experiments was adequately described by the Arrhenius rate equation (Fig. 7). In terms of the Arrhenius coefficients u_∞ and B, this is:

$$u = u_\infty \exp(-B/T). \tag{2}$$

An alternate form in terms of u_{20} and Q_{10} for the temperature interval 20–30° C. is:

$$u = u_{20} Q_{10}^{30{\cdot}32/1-293{\cdot}2°K/T)}. \tag{3}$$

The Arrhenius coefficients and their variances were determined from the linear regression coefficients of $(\ln u)$ on $(1/T)$ by the method of least squares with equal weighting in the transformed data values $(\ln u)$ and $(1/T)$ (Guest, 1961, ch. 6).

u_{20} and Q_{10} and their standard deviations SDu_{20} and SDQ_{10} were in turn calculated from the Arrhenius coefficients as:

$$u_{20} = u_\infty \exp(-B/293{\cdot}2° \text{ K}), \tag{4}$$

$$\text{var}\,(\ln u_{20}) = \text{var}\,(\ln u_\infty) + [(1/293{\cdot}2° \text{ K})^2 - (2/293{\cdot}2° \text{ K})\,(\overline{1/T})]\,\text{var}\,(B), \tag{5}$$

in which var denotes the variance and $(\overline{1/T})$ the mean reciprocal temperature.

SDu_{20} was approximated as:

$$SDu_{20} = u_{20}[\text{var}\,(\ln u_{20})]^{\frac{1}{2}}. \tag{6}$$

From equation (3):

$$Q_{10} = u_{30}/u_{20} = \exp(1{\cdot}125 \times 10^{-4} \text{ °K}^{-1}B), \tag{7}$$

and approximating as in equation (6):

$$SDQ_{10} = Q_{10}(1{\cdot}125 \times 10^{-4} \text{°K}^{-1})[\text{var}\,(B)]^{\frac{1}{2}}. \tag{8}$$

Temperature coefficients and related data were computed with an I.B.M. 7040 digital computer.

RESULTS

Conduction velocities were measured in afferent fibres from 67 tactile spines and 3 proprioceptive campaniform sensilla of group 6, in 16 leg preparations from 12 individuals. Of these, temperature coefficients were determined for 22 tactile spine afferents in 10 preparations from 7 individuals.

Over the 5–42° C. temperature range studied, conduction velocities from 1·0 to 17·4 m./sec. were encountered, ranging 2·2 to 9·0 m./sec. in one preparation (Expt. 13). Five of the receptors failed reversibly at the lower end of the temperature range (Table 2, asterisks), and several failed irreversibly above 35–40° C. With cold failure it was not possible to distinguish between failure of the sensory generator mechanism and failure of conduction. But with heat failure a gradual fall in conduction velocity was sometimes observed during onset, suggesting that conduction failure was involved. However, no attempt was made to study these phenomena systematically, nor to establish limits of the physiological temperature range.

On occasion a slight facilitatory effect of impulse frequency on conduction velocity could be clearly detected on the oscilloscope. During impulse bursts above about 100 sec.$^{-1}$, conduction velocity was increased possibly by as much as 1–5 % in some cases. This incidental observation likewise was not studied further, and the velocity measurements are weighted heavily toward the lower values.

The main results are summarized in Figs. 8 and 9 and Tables 1 and 2. Table 1 presents conduction velocities measured at room temperature only. These were averaged from single readings of several replicate oscilloscope records. In most cases, ten or more replicates were taken; for fewer than ten replicates, standard deviations were not calculated. 'Background discharge', usually spontaneous activity in one or

more fibres other than that from the sensillum under study, occasionally made the crossover points on the oscilloscope records difficult to read. In these cases, the sensillum discharge was identified by waveform, or the records were discarded entirely. This effect was, however, the main source of the occasional larger standard deviations obtained in reading replicate records from a single sensillum.

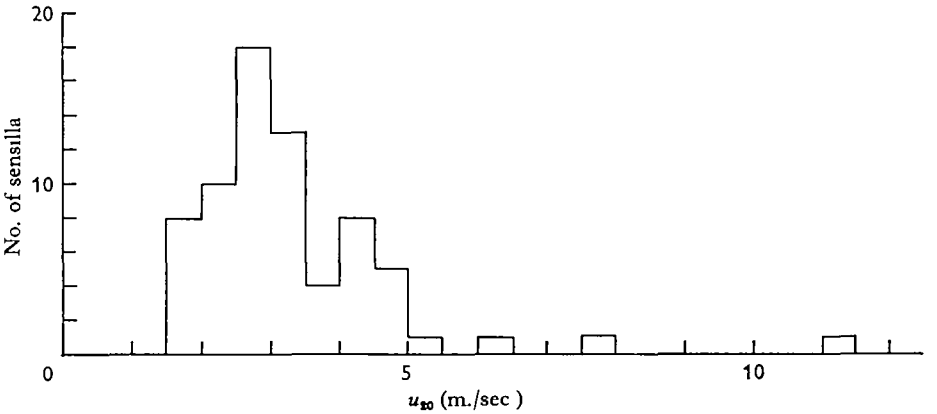

Fig. 8. Histogram of conduction velocities u_{20} (calculated at 20° C.) for all data of Tables 1 and 2, for sixty-seven tactile spines and three proprioceptive campaniform sensilla. Average $u_{20} = 3{\cdot}3 \pm 1\,4$. Range = 1·6–11 0. $n = 70$.

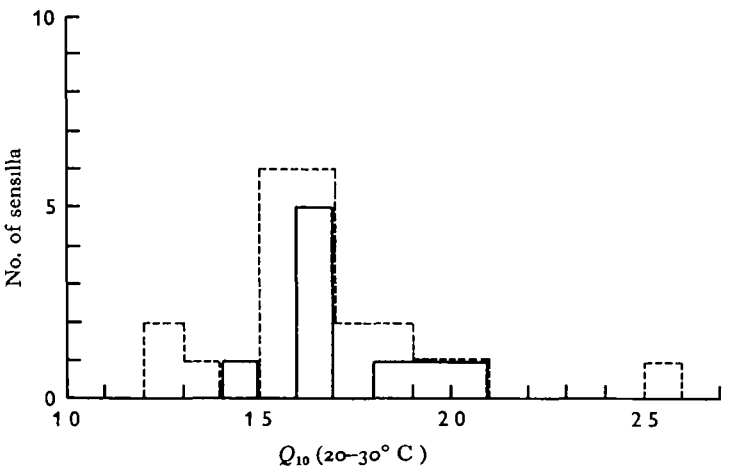

Fig. 9. Histogram of temperature coefficients Q_{10} of conduction velocity, calculated for 20–30° C. Dashed line, values for all twenty-two tactile spines in Table 2; —, values for nine tactile spines from the same series, but calculated using velocities measured at thermal equilibrium only. Average Q_{10} (20–30° C.) = 1·69 ± 0·28. Range = 1·26–2·58. $n = 22$.

The values for u_{20} in Table 1 were estimated for five preparations for which room temperature was recorded, using the average $Q_{10} = 1{\cdot}7$. All these preparations were within a few degrees of 20° C., so that the accuracy of this extrapolation was not critical.

Table 2 presents temperature coefficient data. The Arrhenius coefficients u_∞ and B are significant only to the first two digits, but four digits were carried in computing u_{20} and Q_{10}. The standard deviations of u_∞ and B occur implicitly in those for u_{20} and

Table 1. *Conduction velocities of afferent fibres from* 50 *tactile spines and* 3 *proprioceptive campaniform sensilla, measured at room temperature* (u) *and expressed at* 20° C. (u_{20}) *using* $Q_{10} = 1{\cdot}7$

Expt.	Leg*	Sensillum†	Temperature (°C.)	Conduction velocity (m./sec.) $u \pm$ S.D.	u_{20}
1	L III	PD 5	Not recorded	6·5	—
		PV 3		4·25	—
		PV 4		3·97	—
		PV 5		4·1	—
		PV 6		5·2	—
2	L III	DFS‡	22·5	7·41 ± 0·20	6·45
		D 1‡		4·12 ± 0·11	3·58
		D 2‡		4·72 ± 0·08	4·10
		D 3		5·31 ± 0·10	4·60
		D 4		5·10 ± 0·04	4·43
		PD 3		4·14	3·60
		PD 4		4·13 ± 0·05	3·60
		PD 5		4·96 ± 0·10	4·30
		PV 3		5·19 ± 0·10	4·50
		PV 4		5·26 ± 0 08	4·55
		PV 5		4·64 ± 0·11	4·03
		PV 6		4·81 ± 0·35	4·18
		V		5 28 ± 0·15	4·57
		AV 6		5·04 ± 0·35	4·39
3	R III	DFS‡	24 1	5·31 ± 0·33	4·22
		Gp. 6‡		3·26 ± 0·11	2·59
		Gp. 6‡		3·60 ± 0 09	2·86
		Gp. 6‡		3·40 ± 0·10	2·70
		AD 1‡		3·22 ± 0·14	2·56
		AD 2		3·12 ± 0·14	2·49
		AD 3		3·35 ± 0·12	2·67
		AD 4		3·42 ± 0·10	2·72
		AD 5		3·32 ± 0·14	2·64
		D 1‡		3·49 ± 0·12	2·78
		D 2		2·98 ± 0·15	2·36
		D 3		3·35 ± 0·19	2·67
		D 4		4·00 ± 0·17	3·19
		D 5		3·95 ± 0·24	3·13
		PD 1		3·45 ± 0·18	2·75
		PD 2		3·38 ± 0·08	2·70
		PD 4		3·57 ± 0·14	2·83
		PV 1		2·87 ± 0·08	2·27
		PV 6		2 89 ± 0·26	2·29
		AV 1		2·82 ± 0·04	2·24
		AV 2		2·73 ± 0·10	2·19
		AV 3		2·62 ± 0·12	2·09
		AV 6		2·82 ± 0·20	2·25
4	R III	AD 3	23·9	3·85	3·09
		AD 4	23·9	3·95	3·16
		AD 5	23·3	3·81	3·17
		AD 6	23·3	4·15	3·41
		D 5	23·6	5·04	4·11
		PD 2‡	24·2	3·90	3·08
		PD 3	25·4	4·03 ± 0 04	3·00
		PD 4	23·9	3·84	3·08
		PD 5	23·9	3·85 ± 0·15	3·09
6	L II	AD 3	22·8	3·11	2·65
8	R III	PD 4	24·3	2·72 ± 0·02	2·14

* R, Right; L, left; II, mesothoracic; III, metathoracic.

† DFS, Dorsal femoral spine; Gp. 6, group 6 campaniform sensillum; tibial spines designated by rows as Fig. 2, and numerically from proximal end of each row.

‡ Sensillum was between distal recording electrodes.

Table 2. *Conduction velocities, u_{20}, Arrhenius equation coefficients, u_∞ and B, and Q_{10} for 20 and 30° C., for 22 tactile spine afferent fibres*

(Numbers in parentheses taken from thermally well-equilibrated data only.)

Expt.	Leg	Sensillum	T Range (°C.) Min.	T Range (°C.) Max.	u_∞ (m./sec.)	B (°K.)	$u_{20} \pm$ S.D. (m./sec.)	$Q_{10} \pm$ S.D. (20–30° C.)
5	L III	D 5	7·6	20 9	$3{\cdot}57 \times 10^{9}$	5967	$5{\cdot}17 \pm 0{\cdot}34$	$1{\cdot}96 \pm 0{\cdot}16$
7	L II	AD 4	16·4	24·1	$8{\cdot}16 \times 10^{12}$	8410	$2{\cdot}84 \pm 0{\cdot}12$	$2{\cdot}58 \pm 0{\cdot}35$
		PV 4	16 4	24·1	$7{\cdot}91 \times 10^{9}$	6379	$2{\cdot}81 \pm 0{\cdot}07$ (2·89)	$2{\cdot}05 \pm 0{\cdot}11$ (2·03)
9	L III	AD 6	11·3	29·2	$1{\cdot}36 \times 10^{7}$	4670	$1\ 64 \pm 0{\cdot}04$	$1{\cdot}69 \pm 0{\cdot}07$
		D 5	12·6	23·5	$8{\cdot}44 \times 10^{8}$	4461	$2{\cdot}08 \pm 0{\cdot}02$ (2·05)	$1{\cdot}65 \pm 0{\cdot}04$ (1·65)
		PV 6	12·0	31·8	$2{\cdot}45 \times 10^{8}$	4135	$1{\cdot}84 \pm 0{\cdot}04$ (1·88)	$1{\cdot}59 \pm 0{\cdot}05$ (1·64)
		V	19·3	29·2	$1{\cdot}13 \times 10^{8}$	3938	$1{\cdot}66 \pm 0{\cdot}06$	$1{\cdot}56 \pm 0{\cdot}10$
		AV 5	11·1	24·8	$6{\cdot}47 \times 10^{7}$	5090	$1{\cdot}87 \pm 0{\cdot}04$	$1{\cdot}77 \pm 0{\cdot}06$
		AV 6	11·3	24·8	$2{\cdot}79 \times 10^{8}$	5535	$1{\cdot}76 \pm 0\ 03$ (1·76)	$1\ 86 \pm 0{\cdot}06$ (1·82)
		AV 7	12·4	31·1	$2{\cdot}05 \times 10^{8}$	4071	$1{\cdot}91 \pm 0{\cdot}06$ (1·85)	$1\ 58 \pm 0{\cdot}08$ (1·65)
		A	12 0	23·0	$8{\cdot}56 \times 10^{7}$	5215	$1{\cdot}62 \pm 0{\cdot}01$	$1{\cdot}80 \pm 0{\cdot}02$
10	L III	PD 4	22·9	29·2	—	—	$1{\cdot}99 \pm 0{\cdot}10$	1·36
11	L III	D 5	13·9*	35·0	$2{\cdot}33 \times 10^{8}$	3945	$3{\cdot}34 \pm 0{\cdot}08$	$1{\cdot}56 \pm 0\ 06$
12	R II	AD 3	13·9	36·8	$1{\cdot}80 \times 10^{8}$	3914	$2\ 88 \pm 0{\cdot}05$	$1\ 55 \pm 0{\cdot}03$
		D 3	13 9	35·6	$1{\cdot}72 \times 10^{7}$	4532	$3{\cdot}34 \pm 0{\cdot}09$ (2·80)	$1{\cdot}66 \pm 0\ 06$ (1·60)
13	R III	PD 5	10 0	39·4	$5{\cdot}19 \times 10^{8}$	4130	$3{\cdot}96 \pm 0{\cdot}07$ (3·69)	$1{\cdot}59 \pm 0{\cdot}03$ (1·64)
14	L II	AD 3	9·7*	38·1	$2{\cdot}04 \times 10^{7}$	4610	$3{\cdot}03 \pm 0{\cdot}09$	$1{\cdot}68 \pm 0{\cdot}05$
		AD 4	10·0*	23·8	$1{\cdot}29 \times 10^{8}$	5031	$4{\cdot}58 \pm 0{\cdot}16$	$1{\cdot}76 \pm 0{\cdot}17$
		PD 2‡	11 4*	38·7	$4{\cdot}33 \times 10^{8}$	4163	$2{\cdot}96 \pm 0{\cdot}04$	$1{\cdot}60 \pm 0\ 02$
15	R III	D 3	5·1*	42·0	$1{\cdot}36 \times 10^{4}$	2182	$7{\cdot}96 \pm 0{\cdot}33$ (7·37)	$1{\cdot}28 \pm 0{\cdot}05$ (1·42)
		D 4	11 3	35·6	$1{\cdot}16 \times 10^{4}$	2041	$11{\cdot}04 \pm 0{\cdot}41$	$1{\cdot}26 \pm 0{\cdot}05$
16	L III	D 5	10·8	24 3	$2{\cdot}30 \times 10^{7}$	4654	$2{\cdot}94 \pm 0{\cdot}06$ (2·96)	$1{\cdot}69 \pm 9\ 07$ (1·93)

* Blocking temperature.

‡ Sensillum was between distal recording electrodes.

Q_{10} (equations 5, 6, 8). As indicated in equation (5), the standard deviation of $\ln u$ calculated at other than 20° C. goes through a broad minimum at $\overline{(1/T)}$, the mean reciprocal temperature of the data points. Since the corresponding mid-range temperature was usually near 20° C., u_{20} lies in the region in which calculated conduction velocity can be most precisely specified (Fig. 7).

With nine sensilla, possible artifacts due to thermal non-equilibrium were considered. These were cases in which, due to the nature of the method of varying the temperature, a number of values were taken after relatively long periods when the temperature had been changing very slowly. Usually this happened in trying to reach the extreme upper and lower limits of the range. For these cases Arrhenius coefficients were recalculated using only points for which chamber temperature had changed by less than a degree during the previous 2–3 min. at two or more representative regions of the temperature range. The corresponding 'well equilibrated' values of u_{20} and Q_{10} are tabulated in parentheses below those determined using all of the data values. In most 'well equilibrated' cases the coefficients are within one standard deviation of the original estimates, and it may be concluded that the thermal response of the temperature chamber and the data sampling method were adequate.

All of the estimates of u_{20} are plotted as a histogram in Fig. 8. The distribution appears to be unimodal, and somewhat skew. The mean and standard deviation for the seventy sensory afferent fibres, $3{\cdot}3 \pm 1{\cdot}4$ m./sec., indicate a rather broad natural variation, of the order of half the mean, for the population of fibres studied. It is however, appreciably less than the 3- to 4-fold changes due to temperature over the physiological temperature range.

The values of Q_{10} are likewise given as a histogram in Fig. 9. The dashed lines indicate the distribution found for all twenty-two sensilla using all of the data; the solid line is plotted only for the 'well equilibrated' data of the nine fibres so indicated in Table 2. The 'well equilibrated' values are distributed like the total data set, confirming the earlier conclusion that thermal lag was not a serious problem. The mean Q_{10}, $1{\cdot}7 \pm 0{\cdot}3$, agrees with the classic value 1·79 of Keith Lucas (1908) for frog sciatic nerve.

DISCUSSION

Wavelength of the action potential. The length and shape of the action potential has a bearing on the accuracy of the velocity estimate. The total wavelength L of the longitudinal action current was estimated from the total duration τ of the diphasic action potential, the inter-electrode spacing s across which it was observed, and the conduction velocity, u, from the relation:

$$L = \tau u - s. \tag{9}$$

To a first approximation the length L_a of the active region of fibre membrane, in which the membrane action current is inward, can be estimated from the relative duration of the time-interval between the negative and positive peaks of the diphasic action potential, as:

$$L_a = L\tau_a/\tau. \tag{10}$$

For the experiment shown in Fig. 10, average total and active-region wavelengths were 2·4 mm. and 1·3 mm. respectively, and were essentially invariant with temperature over the entire range. Comparable wavelengths and temperature independence

were found in twenty-four afferent fibres examined. These short wavelengths are consistent with the short length constants, about 1 mm. for the faster-conducting giant fibres of the ventral nerve cord of *Periplaneta* (Yamasaki & Narahashi, 1959*b*). Clearly the 2–4 mm. inter-electrode spacing in these experiments was not negligible compared with the wavelength of the action potential. Possible errors thus introduced are discussed later. Likewise the diameter of the tissue space in leg segments is not negligible compared with the wavelength, so that volume conduction must be important *in situ*.

Accuracy considerations. The precision of the graphical method for reading reciprocal conduction times from oscilloscope records was about 3–4 %. The accuracy of the measurement of conduction distance now needs to be considered, since any

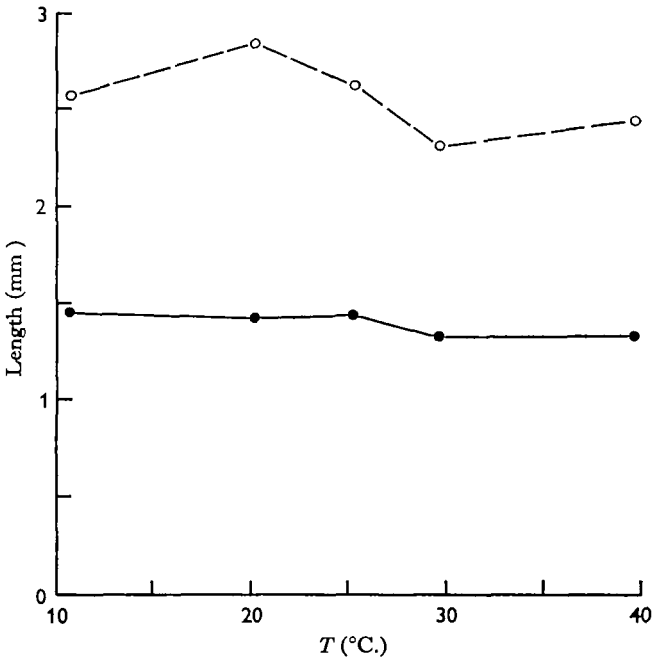

Fig. 10. Length of the propagated disturbance as a function of temperature. O, Estimated for total length of the diphasic action potential; ●, estimated for the inwardly directed radial current (Expt. 13).

errors introduced by it have been neglected in the tabulated data. Two points are involved: (1) the anatomical measurement and (2) the interpretation of the baseline-crossing interval.

The estimated lengths of conduction path between the two pairs of recording electrodes were typically 10 mm., ranging roughly from 7 to 15 mm. for all the preparations studied. The largest uncertainty arose in measuring around the flexed femoro-tibial joint, and was typically $\pm 0{\cdot}5$ mm., or of the order of 3–8 %. For any given leg preparation, the anatomical uncertainty is a systematic error, constant for those sensilla below the distal electrode pair, and constant over the range of temperature. However, it is not systematic with respect to the group of leg preparations studied. Moreover, it affects the calculated conduction velocities proportionately, and therefore does not enter the estimate of Q_{10}.

The baseline-crossing problem deals with establishing the beginning and end points of the conduction path, in terms of the position of an impulse relative to the pair of recording electrodes at which a baseline crossing is observed. Two contributing factors are: (1) in the usual electrode configuration used, the inter-electrode spacings were unequal and were appreciable fractions of the conduction distance; (2) many of the recorded wave forms of the action potential were appreciably irregular. For an action potential of 'regular' waveform, if the magnitude of the leading longitudinal action current is twice that of the trailing, then the peak of the membrane action potential will be about two-thirds of the way through the inter-electrode distance at the moment when the two recording electrodes are in equipotential, i.e. at a baseline crossing. True conduction distance thus differs from the assumed inter-midpoint distance by one-sixth of the spacing difference. With unequal spacings of 2 mm. and 4 mm., and with the widely spaced pair always proximal, i.e. the second set encountered, the true path length is greater than the inter-midpoint distance by $\frac{1}{3}$ mm. Even if the ratio of longitudinal currents were as high as 3:1, as for the giant fibres in the ventral nerve cord of *Periplaneta* in sodium-enriched media (Yamasaki & Narahashi, 1959*a*), the error would still be only $\frac{1}{2}$ mm. To the extent that the wavelength and the shape of the impulse in each fibre is temperature-independent, this error (like the anatomical one), does not affect the Q_{10}. It does affect the conduction velocity proportionately as the path length, such that for those electrode configurations as in Fig. 1, the true conduction velocities are 3–5 % higher than the tabulated values.

Action potentials with irregular waveforms are more difficult to deal with. Our data do not distinguish between deviations from simple wave propagation of the membrane mechanism, and effects arising from non-uniform extra-axonal conductance in the inter-electrode space. No attempt has been made to estimate errors arising from non-uniform conduction of axonal origin, nor to deal with other than simple extra-axonal irregularities. It is virtually certain that the cross-sectional area of the extra-axonal tissue everywhere *in situ* is at least 100 times the intra-axonal, so that the extra-axonal conductance probably does not limit impulse propagation. However, large changes in extracellular conductance occurring in an inter-electrode space, as at the femoro-tibial and trochanteral joints, change the potential gradients in the extra-axonal medium, and hence shift the positions of equipotential points relative to the peak of the impulse (Marmont, 1940). This problem arose in the minority of preparations in which the electrode pairs immediately across those joints were used. The cross-sectional area of the upper tibial lumen is about a tenth that of the femur, so that the joint presents ascending impulses with a tenfold conductance increase. The increase across the trochanter is probably similar. For a 2:1 longitudinal action current ratio, and 4 mm. inter-electrode spacing, a tenfold step increase in conductance midway along the the inter-electrode space would shift the impulse peak ahead to about four-fifths the distance between equipotentials. The peak of the impulse would then be 0·3 mm. beyond the midpoint at the crossover instant (neglecting effects arising because the wavelength is less than the inter-electrode spacing in these cases). With this electrode configuration, however, similar effects occur at both electrode pairs, since the two inter-electrode spacings were nearly equal, and the effects of these two systematic errors in estimating the conduction distance are largely cancelled.

A special problem arises with the afferent of the dorsal femoral spine and those of

the group 6 campaniform sensilla and of the upper tibial spines, as these sensilla lay on the distal inter-electrode space (Tables 1 and 2, ‡). While we have not attempted to estimate the impulse position relative to the distal electrode pair at the moment of the distal baseline crossing, it seems likely that the true conduction distance was less than the distance between midpoints by not more than half the distal inter-electrode spacing. The true conduction velocities of these fibres may be as much as 10–20% lower than calculated.

It is unlikely that the cut proximal end of the nerve trunk presents a conduction problem in most cases, since the most proximal recording electrode was usually several millimeters from the cut end. The length constant of these fibres can be estimated from the data of Boistel & Corabœuf (1954) and Yamasaki & Narahashi (1959*b*) for *Periplaneta* giant fibres (conduction velocity = 7 m./sec. and length constant = 1 mm. respectively) and the conclusion from local circuit theory that length constant and conduction velocity are proportional. Thus length constants in these afferents should be about half those of giant fibres, or 0·5 mm., so that the last recording electrode was probably 5–10 length constants from the cut end in most cases. The two fastest axons (Table 2, Expt. 15) are also those with the lowest Q_{10}'s, suggesting the possibility that the fibres were damaged with decremental conduction toward the more proximal electrode pair. However, there was no direct evidence of damage, and these fibres did continue to conduct as long as many of the others, so that the data have not been rejected.

To summarize the random and systematic errors attributable to the limits of graphical precision, anatomical length measurement, and electrode placement effects, the relative error in an individual determination of conduction velocity, taken simply as the sum of the individual relative errors, is about 3 ± 6% to 5 ± 12% for preparations with unequal inter-electrode spacing, or ± 6–12% for those with equal spacing. These experimental errors are appreciably smaller than the population variability for conduction velocity.

Fibre diameters. No direct measurements of fibre diameter were undertaken in the present work, but it is useful to estimate diameters of these afferent fibres by comparing our results with data in the literature. Fig. 11 and Table 3 collate data from several insect species, in which velocities range from among the fastest found in insects to significantly below those studied here. In most cases, the diameter measurements and velocity measurements have been made by different authors, and frequently temperatures have not been specified. The entire collection of data does, however, agree plausibly with the theoretical parabolic relation between velocity and diameter D,

$$u = kD^{\frac{1}{2}} \tag{11}$$

(Fig. 11, dashed curve), of Pumphrey & Young (1938), Hodgkin (1954) and others, for unmedullated nerve. Within the limits of this comparison, our values of conduction velocity indicate fibre diameters of the order of 10 μ, ranging from about 3 to 20 μ within one standard deviation of the mean velocity for the population. This physiological estimate thus agrees with Pringle's (1938) measurements of 6–15 μ for afferent fibres from campaniform sensilla in the trochanter, and does not support Guthrie's (1962) conclusion that in the legs of *Periplaneta* only motor fibres exceed 5 μ.

Non-correlation with sensory path length. The possible correlation of conduction

velocity and distance from the sensillum to the thoracic ganglion was examined in one preparation (Table 1, Expt. 3) in which a large number of sensilla were studied. The results were clearly negative (Fig. 12). Linear correlation coefficients for the tibial dorsal row of spines (D 1–5), the anterio-dorsal row (AD 1–5) and for all spines were 0·73, 0·70 and 0·13 respectively, with respective chance occurrence probabilities (p values) 0·19, 0·26 and 0·73. Accordingly, there is no peripheral compensation for conduction distance in these nerve fibres, such as is found in the giant fibre system of the squid mantle (Pumphrey & Young, 1938) where rather precise compensation for conduction time is utilized in motor co-ordination.

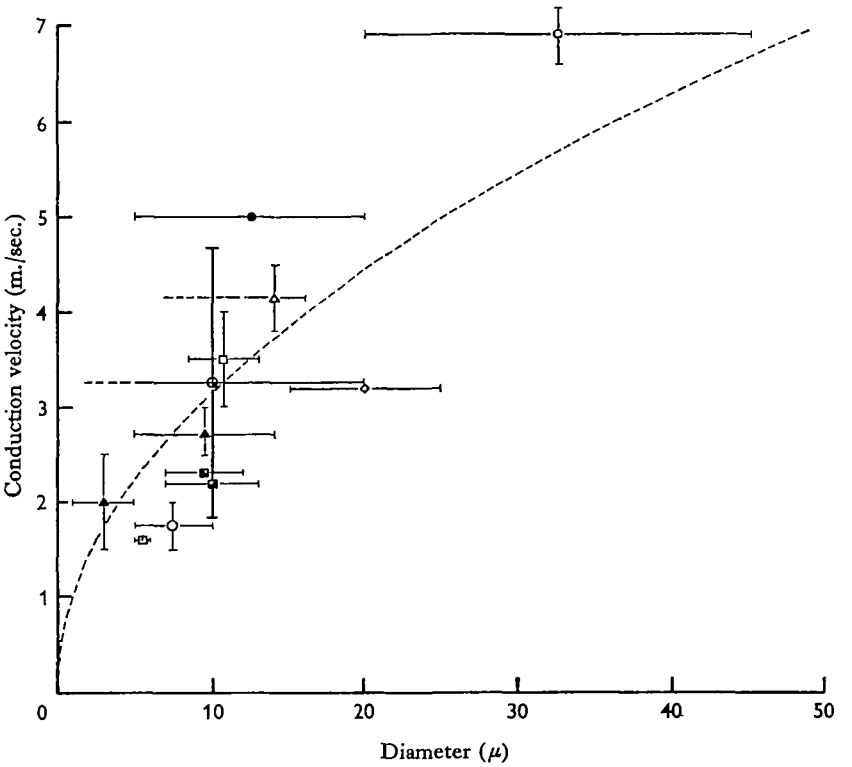

Fig. 11. Conduction velocity as a function of fibre diameter for several types of insect nerve, collating various estimates. Dashed curve, $u = kd^{\frac{1}{2}}$, arbitrarily assigning $k = 1$ m.sec.$^{-1}\mu^{-\frac{1}{2}}$. Conduction velocities have been expressed as at 20° C. if possible, using $Q_{10} = 1{\cdot}7$ if necessary. Vertical bars indicate standard deviation if available, or range; horizontal bars indicate range where stated, dashed left end indicating continuous distribution into small diameters. Legend: see Table 3.

Effects of conduction delay on the sensory transfer function. Sensory transfer functions are potentially useful both in identifying time-dependent transduction processes at the sensory ending, and in describing the code with which information is conveyed. Conduction delay has a bearing on both points; it must not be confused with transduction processes, and it must be recognized as a component of the sensory code.

The sensory transfer functions of Pringle & Wilson (1952) and Chapman & Smith (1963) were not corrected for conduction delay. The effect of introducting a simple time delay, t, between the input and output of a linear system with transfer function $F(s)$

Table 3. *Conduction velocities and fibre diameters in several larger insects (see Fig. 11)*

Symbol (Fig. 11)	Nerve fibre	u^* (m./sec)	Diameter (μ)	Reference
	Periplaneta			
○	Connective giant	6·6–7·2	—	Boistel & Corabœuf (1954)
		—	20–45	Roeder (1948)
●	Connective smaller large fibre	5	5–20	Roeder (1948)
⊙	Cercal afferent	2·0–3·0	5–10	Roeder (1953)
⊕	Tactile spine, c.s. afferent	3·3 ± 1·4	—	This paper
	5th podial nerve	—	< 5–20	Guthrie (1962)
	Trochanter c s. afferent	—	6–15	Pringle (1938)
	Locusta			
□	Connective giant	3–4	—	Fielden (1960)
		—	8·5–13	Cook (1951)
◪	Extensor tib. fast motor	2·2	10–13 × 7–9	Hoyle (1955)
◩	Extensor tib. slow motor	2·3	9–12 × 7–8	Hoyle (1955)
⊡	Extensor tib. third axon	1·6	5–6	Hoyle (1955)
	Schistocerca			
◇	Flight fast motor	3·2	15–25	Neville (1963)
	Anax			
△	Connective giant	3·8–4·5	—	Fielden (1960)
		—	< 5–16	Hughes (1953)
▲	Paraproct efferent	2·5–3·0	5–14	Fielden (1960)
△	Paraproct afferent	1·5–2·5	1–5	Fielden (1960)

* Corrected to 20° C. where possible, using $Q_{10} = 1{\cdot}7$.

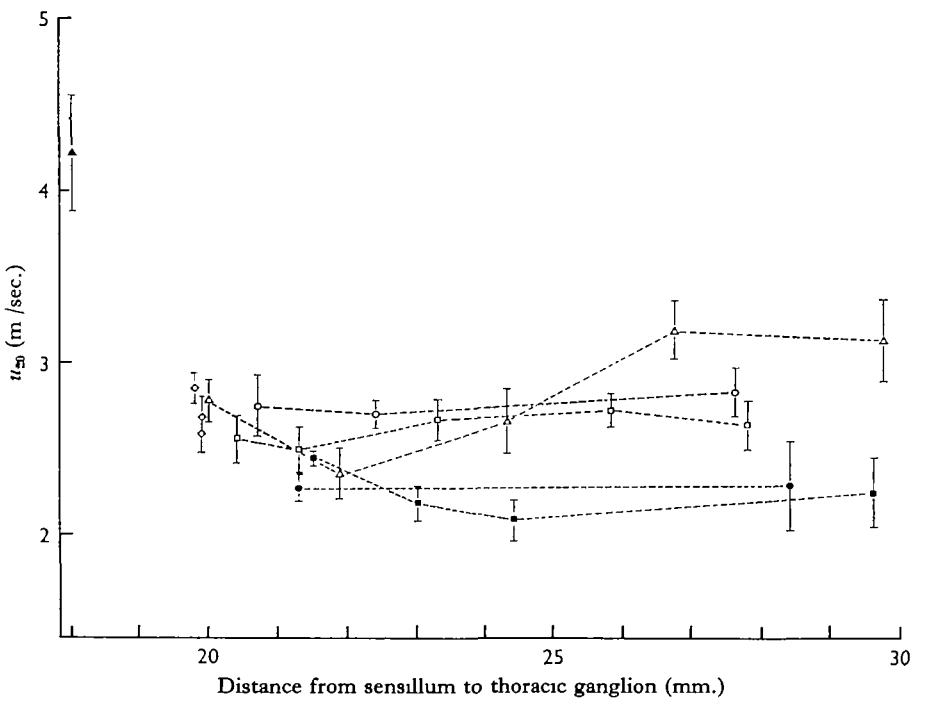

Fig. 12. Conduction velocities as functions of the estimated distance from the sensillum to the thoracic ganglion, for nineteen tibial tactile spines, the dorsal femoral spine (DFS), and for three proprioceptive campaniform sensilla of group 6. Sensilla of Table 1, Expt. 3. ○, PD; △, D; □, AD; ■, AV; ●, PV; ▲, DFS; ◇, gp. 6.

(defined by Laplace transforms) is well known*; the transfer function with delay becomes $F(s)\exp(-ts)$. In terms of the frequency response function, obtained by evaluation with the imaginary values of the complex frequency s,

$$s = 0 + j2\pi f, \tag{12}$$

the delay factor becomes

$$\exp(-ts) = \exp(-j2\pi ft). \tag{13}$$

For a sinusoidal input with frequency f the delay factor simply shifts the phase of the corresponding output sinusoid by phase angle

$$\phi = -2\pi ft, \tag{14}$$

and has no effect on its amplitude.

In the present case, when a sensory discharge has been monitored at a distance d from the sensillum, the transfer function relating the observed impulse-frequency modulation to a mechanical input contains implicitly the conduction delay factor

$$\exp(-ts) = \exp(-sd/u), \tag{15}$$

with corresponding phase shift

$$\phi = -2\pi f(d/u). \tag{16}$$

For the average conduction velocity, $u_{20} = 3{\cdot}3$ m./sec., the phase-shift per unit conduction distance and unit sinusoidal input frequency is

$$\phi/fd = -0{\cdot}11°/\text{mm. (cycle per sec.)}. \tag{17}$$

Since the phase-shift varies inversely with conduction velocity, its Q_{10} is the reciprocal of that for conduction velocity, or about 0·6.

In the transfer function experiments of Chapman & Smith (1963) on the dorsal femoral spine preparation, the recording electrodes were usually about 5 mm. from the sensillum, and the latter gave frequency-modulated discharges for input sinusoids from about 0·01 to 30 cycle/sec. This gives the phase-angle correction, by which the transfer function at the sensillum leads the observed values, as about

$$-\phi/f = +0{\cdot}55°/\text{cycle per sec.}, \tag{18}$$

or about 16° at 30 cycle/sec. While it is well within the limits of precision of measured transfer functions over most of the physiological frequency range, the effect is not negligible at the uppermost frequencies.

In the time domain, the conduction delay per unit distance is simply the reciprocal of velocity. For $u_{20} = 3{\cdot}3$ m./sec. it is 0·3 msec./mm. Like the phase shift, it has a Q_{10} of about 0·6. In keeping with linear transfer-function theory as well as with intuition, it does not appreciably distort the sequence of impulses originating at the sensillum, but merely delays its presentation to the central nervous system. A minor facilitatory effect of impulse frequency on conduction velocity has been mentioned earlier, and to this extent the waveform of modulated impulse frequency is slightly peaked at high impulse frequencies. But it is likely that, in at least some circumstances, the temporally encoded signal from these sensilla is transmitted with precision well beyond its meaningful information content. Wilson & Gettrup (1963) and Wilson (1966) have suggested that in insect flight and running, volleys of proprioceptive impulses serve mainly to regulate the timing of central endogenous oscillators, and

* A biologically oriented treatment of this subject is given by Milsum (1966); Aseltine (1958) gives further detail.

do not participate directly in the precise control of movements. It remains to be shown, however, how much of the available sensory information is actually utilized in walking and in other more delicate motor acts such as leg preening.

Among the tactile spines, since conduction velocity is uncorrelated with path length, the main effect of the spatial distribution of sensilla is probably merely to increase the dispersion of conduction delays. For fibres within one standard deviation of mean u_{20} conduction delays vary 2- to 3-fold due to the velocity distribution. The range of sensory path lengths from the most proximal of the ventral femoral spines to the most distal tibial spines, about 10–30 mm., increases the spread by another factor of 3, so that corresponding delays range from about 2 to 15 msec. As with temporal encoding, however, it seems unlikely that conduction delay effects limit any known behavioural reactions involving sensory input from tactile spines.

In proprioception, however, conduction delays may be closely matched to the fastest locomotor responses. Wilson (1965) has measured minimum reflex latencies for proprioception in cockroach legs of 10 msec. or less, from mechanical input to the first 'muscle potential', in muscles whose oscillatory periods may approach 50 msec. in rapid running. If our velocity data are valid for the major groups of proprioceptive campaniform sensilla, it is clear that only the most proximal groups can participate in the fastest reflex phenomena. Conduction times in fibres within one standard deviation of mean u_{20} range from 5 msec. or less from even the slower fibres of trochanteral and upper femoral groups 1–5 to well beyond 8 msec. for even the faster fibres from tarsal sensilla. If synaptic delay and motor transmission occupy about half the minimum latency, then most of the group 1–5 sensilla, but only about half those of group 6 on the upper tibia, can report in time; almost all the tarsals must be excluded. However, Wilson (1965) points out that muscle contraction, not minimum reflex latency, is probably what limits stepping frequencies in fast running. Evidently then, with stepping periods of 50 msec. and longer, nearly all of the proprioceptive input arrives at the thoracic ganglion well within a single period. Whatever role proprioceptive information may have in locomotion, it seems that most of it could be available for fairly simple reflex effects.

SUMMARY

1. Conduction velocities of individual afferent nerve fibres from tactile spines and proprioceptive campaniform sensilla have been measured *in situ* over the temperature range 5–42° C., in leg preparations of the cockroach *Periplaneta americana*.

2. Conduction velocities at 20° C. (u_{20}) averaged $3{\cdot}3 \pm 1{\cdot}4$ m./sec., ranging from 1·6 to 11·0 m./sec.

3. Temperature coefficients, expressed as Q_{10} for the interval 20–30° C., averaged $1{\cdot}7 \pm 0{\cdot}24$, ranging from 1·3 to 2·6.

4. The length of the propagated disturbance is about 2–3 mm., and is nearly temperature-independent.

5. Fibre diameters, estimated from conduction velocity, must be about 10 μ.

6. There is no correlation between conduction velocity and distance from the sensillum to the thoracic ganglion. Conduction delays in fibres conducting within one standard deviation of mean u_{20} range from about 2 to 15 msec., from the most proximal to the most distal tactile spines.

7. The effect of conduction delay on temporal and spatial sensory encoding is probably unimportant from a behavioural point of view. It contributes a factor of the form $\exp(-sd/u)$ to the sensory transfer function, and may be appreciable at upper physiological frequencies of impulse frequency modulation.

We thank Drs J. M. Marshall and B. T. and P. A. Stewart for criticizing the manuscript, and Messrs J. Mares and N. Allahar for technical assistance.

REFERENCES

ASELTINE, J. A (1958). *Transform Method in Linear System Analysis.* New York, Toronto, London: McGraw-Hill.

BOISTEL, J. & CORABŒUF, E. (1954). Potentiel de membrane et potentiels d'action de nerf d'insects recueillis à l'aide de microélectrodes intracellulaires. *C. r. hebd. Séanc. Acad. Sci., Paris* **238**, 2116–18.

BULLOCK, T. H. & HORRIDGE, G. A. (1965). *Structure and Function in the Nervous Systems of the Invertebrates.* San Francisco and London: Freeman.

CHAPMAN, K. M. (1957). A miniature direct-plotting pulse-frequency nomogram. WADC TN 57–371, ASTIA Document no. 142 097, Wright Air Development Center, Wright-Patterson Air Force Base, Ohio, U.S A.

CHAPMAN, K. M. (1965). Campaniform sensilla on the tactile spines of the legs of the cockroach. *J. exp. Biol.* **42**, 191–203.

CHAPMAN, K. M. & SMITH, R. S. (1963). A linear transfer function underlying impulse frequency modulation in a cockroach mechanoreceptor. *Nature, Lond.* **197**, 699–701.

COOK, P. M. (1951). Observations of giant fibres of the nervous system of *Locusta migratoria*. *Q. Jl Microsc. Sci.* **92**, 297–305.

DRESDEN, D. & NIJENHUIS, E. D. (1958). Fibre analysis of the nerves of the second thoracic leg in *Periplaneta americana*. *Proc. K. ned. Akad. Wet.* C **61**, 213–23.

FIELDEN, A. (1960). Transmission through the last abdominal ganglion of the dragonfly nymph, *Anax imperator*. *J. Exp. Biol.* **37**, 832–44.

GUEST, P. G. (1961). *Numerical Methods of Curve Fitting.* Cambridge University Press.

GUTHRIE, D. M. (1962). Regenerative growth in insect nerve axons. *J. Insect Physiol.* **8**, 79–92.

HODGKIN, A. L. (1954). A note on conduction velocity. *J. Physiol.* **125**, 221–24.

HOYLE, G. (1955). The anatomy and innervation of locust skeletal muscle. *Proc. R. Soc.* B, **143**, 281–92.

HUGHES, G. M. (1953). 'Giant' fibres in dragonfly nymphs. *Nature, Lond.* **171**, 87–8.

LUCAS, K. (1908). The temperature coefficient of the rate of conduction in nerve. *J. Physiol.* **37**, 112–21.

MARMONT, G. (1940). Action potential artefacts from single nerve fibers. *Am. J. Physiol.* **130**, 392–402.

MILSUM, J. H. (1966). *Biological Control Systems Analysis.* New York, Toronto, London: McGraw-Hill.

NEVILLE, A. C. (1963). Motor unit distribution of the dorsal longitudinal flight muscles in locusts. *J. Exp. Biol.* **40**, 123–36.

NIJENHUIS, E D. & DRESDEN, D. (1952). A micromorphological study on the sensory supply of the mesothoracic leg of the American cockroach *Periplaneta americana*. *Proc. K. ned. Akad. Wet.* C, **55**, 300–10.

PRINGLE, J. W. S. (1938). Proprioception in insects. II. The action of the campaniform sensilla on the legs. *J. Exp. Biol.* **15**, 114–31.

PRINGLE, J. W. S. & WILSON, V. J. (1952). The response of a sense organ to a harmonic stimulus. *J. Exp. Biol.* **29**, 220–34.

PUMPHREY, R. J. (1936). Slow adaptation of a tactile receptor in the leg of the common cockroach. *J. Physiol.* **87**, 6*P*

PUMPHREY, R. J. & YOUNG, J. Z. (1938). The rates of conduction of nerve fibres of various diameters in cephalopods. *J. Exp. Biol.* **15**, 453–66.

ROCKSTEIN, M. (1965). *The Physiology of Insecta*, vol. II. New York: Academic Press.

ROEDER, K. D. (1948). Organization of the ascending giant fiber system in the cockroach (*Periplaneta americana*). *J. Exp. Zool.* **108**, 243–61.

ROEDER, K. D. (1953). Electrical activity in nerves and ganglia. In *Insect Physiology* (ed. K. D. Roeder), ch. 17. New York: Wiley.

TREHERNE, J. E. & BEAMENT, J. W. L. (1965). *The Physiology of the Insect Central Nervous System.* New York: Academic Press.

WILSON, D. M. (1965). Proprioceptive leg reflexes in cockroaches. *J. Exp. Biol.* **43**, 397–410.

WILSON, D. M. (1966). Insect walking. *Am. Rev. Entom.* **11**, 103–22.

WILSON, D. M. & GETTRUP, E. (1963). A stretch reflex controlling wingbeat frequency in grasshoppers. *J. Exp. Biol.* **40**, 171–85.

YAMASAKI, T. & NARAHASHI, T. (1959*a*). The effects of potassium and sodium ions on the resting and action potentials of the cockroach giant axon. *J. Insect. Physiol.* **3**, 146–58.

YAMASAKI, T. & NARAHASHI, T. (1959*b*). Electrical properties of the cockroach giant axon. *J. Insect. Physiol.* **3**, 230–42.